A new methodology for the assessment of climate change impacts on a watershed scale

Slobodan P. Simonovic

Department of Civil and Environmental Engineering, The University of Western Ontario, London, Ontario, Canada, N6A 5B9

Many climate change impact studies have been conducted using a top-down approach. First, outputs from global circulation models (GCMs) are considered which are downscaled in a second step to the river basin scale using either a statistical/empirical or a dynamic approach. The local climatic signal that is obtained is then used as input into a hydrological model to assess the direct consequences in the basin. Problems related to this approach include: a high degree of uncertainty associated with GCM outputs and an increase in uncertainty due to the downscaling approach. An inverse approach is proposed in this article to improve the understanding of the processes leading to hydrological hazards including both flood and drought events. The approach analyses of existing guidelines and management practices in a river basin with respect to critical hydrological exposures that may lead to failure of the water resources system or parts thereof. Critical hydrologic exposures (flood levels for example) are then transformed into corresponding critical meteorological conditions (extreme precipitation events for example). These local weather scenarios are then statistically linked to possible large-scale climate conditions that are available from the GCMs. The proposed procedure allows for the assessment of the vulnerability of river basins with respect to climate forcing. It also provides a tool for identifying the spatial distribution of the vulnerability and risk.

Keywords: Climate change, global circulation models, impact assessment, watershed, water resources.

Introduction

THE potential impacts of climate change on hydrological extremes have received considerable attention from hydrologists during the last decade. Many studies suggest that global warming will increase the frequency and magnitude of extreme hydrological events[1,2]. According to IPCC[3], flood magnitude and frequency are likely to increase in most regions, and low flows are likely to decrease in many regions of the world. Climate change may also alter the timing of extreme runoff. Hansen *et al.*[4] reported that changing the air temperature by only 2–4°C can have a significant impact on snow accumulation and melt rate. Satellite data show a decrease of about 10% in the extent of snow cover since the late 1960s (ref. 5).

In many areas where snowfall is currently an important component of the water balance, river peak flow is likely to move from spring to winter[6,7]. Because of its location, Canada is projected to experience greater rates of warming than many other regions of the world. According to Lemmen and Warren[8], changes in Canadian climate will be variable across the country, with the Arctic and the southern and central Prairies expected to warm the most. The average air temperature in Canada has risen by 1.1°C in the past century[9]. Although Canada has a relative abundance of water, it is not evenly distributed across the country. As a result, most regions it experience water-related problems, such as floods, drought and water quality deterioration. Therefore, water resources is one of the highest-priority area with respect to climate change impacts and adaptation in Canada[8].

Climate in Canada is generally warmer and wetter during the last half of the twentieth century. Gan[10] found significant warming particularly in January, March, April, May and June over the last 40 years in western Canada. Whitfield and Cannon[11] compared meteorological data for two different decades, and found the more recent decade to be generally warmer. According to Zhang *et al.*[12], the annual average air temperature exhibits an increasing trend in southwestern Canada and a decreasing trend in northeastern Canada. They found that the annual precipitation have changed by –10% to 35%. The authors have identified significant decreasing trends in winter precipitation and in the proportion of spring precipitation falling as snow in southeastern Canada. Frequency and magnitude of extreme precipitation is also predicted to change in Canada. For example, Zwiers and Kharin[13] estimated that under a $2\times CO_2$ scenario, the return period of extreme precipitation would be shortened by half in Northern Canada. Changes in Canadian river flow correspond broadly to the regional changes identified in Canadian climate. Zhang *et al.*[14] calculated trends for 11 hydrometric variables for various Canadian catchments and found generally decreasing trends in river flow volumes, particularly in August and September. Significant increases in March and April river flows were observed. Snowmelt is an important source of river runoff and a significant flood-producing mechanism in many parts of

e-mail: simonovic@uwo.ca

Canada. Mote[15] found evidence of warming-induced snow-pack declines, around 30% since 1950, particularly in spring and at lower elevations in the Georgia Basin–Puget Sound region.

Changes in the frequency of hydro-climatic extremes may be one of the most significant consequences of climate change. Studies show that the overall flood magnitude and frequency of occurrence would increase in the coastal basin, and decrease in the interior basin. Roy *et al.*[16] studied the impact of climate change on summer and fall flooding on the Chateauguay River Basin (Quebec, Canada). The authors indicated potentially serious increases in the volume of runoff, maximum discharge and water level under future climate change scenarios.

Droughts are also projected to become severe in Canada. Hengeveld[17] projected more frequent occurrence of droughts. The drought of 2001 affected Canada from coast to coast, with significant economic and social impacts. Many areas experienced the lowest summer precipitation[8]. In 2001, the level of Great Lakes reached its lowest point in more than 30 years[18]. Significant trends towards longer frost-free periods could increase drought occurrence since longer ice-free season for lakes and rivers increases the potential for open-water evaporation[19].

Most hydrological studies use the so-called impact approach to assess the potential consequences of climate change to the basin river runoff. This study attempts to improve our understanding of the processes leading to local hydrologic hazards by introducing an inverse (or bottom-up) approach to the modelling of flood risk and vulnerability to changing climatic conditions[20–22]. Proposed methodology has been implemented in the Upper Thames River basin (UTRB) in southwestern Ontario, Canada. The main purpose of this article is to provide methodological details of the approach and offer guidelines for its implementation.

Methodology

The inverse impact modelling approach is aimed at assessing the vulnerability of river basin hydrologic processes to climate forcing from a bottom-up perspective. The approach consists of the following four steps.

Step 1. Identification of critical hydrologic exposures that may lead to local failures of water resource systems in a particular river basin. Critical exposures are analysed together with existing guidelines and management practices. Vulnerable components of the river basin are identified together with the risk exposure. The water resource risk is assessed from three different viewpoints: risk and reliability (how often the system fails), resiliency (how quickly the system returns to a satisfactory state once a failure has occurred) and vulnerability (how significant are the likely consequences of a failure). This step is accomplished in collaboration with local water authorities.

Step 2. In the next step, the identified critical hydrologic exposures (such as floods and droughts) are transformed into corresponding critical meteorological conditions (e.g. extreme precipitation events, sudden warming, prolonged dry spells). A hydrologic model is used to establish the inverse link between hydrologic and meteorological processes. Reservoir operation, floodplain management and other anthropogenic interventions in the basin are also included in the model. In this study, the US Army Corps of Engineers (USACEs) Hydrologic Engineering Centre Hydrologic Modelling System (HEC-HMS) is used to transform inversely extreme hydrologic events into corresponding meteorological conditions. HEC-HMS is a precipitation–runoff model that includes a large set of mix-and-match methods to simulate river basin, channel and water control structures.

Step 3. A weather generator (WG) is used to simulate the critical meteorological conditions under present and future climatic scenarios. The WG produces synthetic weather data that are statistically similar to the observed data. Since the focus is mainly on extreme hydrologic events, the generator reflects not only the mean conditions, but also the statistical properties of extreme meteorological events. The K-NN algorithm is used to perform strategic resampling to derive new daily weather data with altered mean or variability. In the strategic resampling, new weather sequences are generated from the historical record based on prescribed conditioning criteria. For a given climatic variable, regional periodical deviations are calculated for each year and for each period.

Step 4. In the final stage, the parameters of the WG are linked with global circulation models (GCM) and an ensemble of simulations reflecting different future climatic conditions is generated. The frequency of critical meteorological events causing specific water resources risks is then assessed from the WG outputs.

The main advantages of the inverse approach over the traditional top-down approach are: (i) a focus on specific existing and potential water resource problems; (ii) a direct link with the end user and (iii) easy updating, when new and improved GCM outputs become available.

Hydrologic modelling

In this study, the US Army Corps of Engineers (USACE) Hydrologic Engineering Center Hydrologic Modeling System (HEC-HMS) is used to inversely transform extreme hydrologic events into corresponding meteorological conditions. HEC-HMS is a precipitation–runoff model that includes a large set of mix-and-match methods to simulate river basin, channel and water control structures. It is designed for application to a wide range of geographic areas for solving a variety of hydrologic problems[23]. The model has been applied successfully in numerous studies.

An event-version of the HMS model can be used for simulating short rainfall–runoff events and is used in this study for the analysis of high flow events that can cause flooding in the basin. The structure of the event HMS model comprises six components describing main hydroclimatic processes in the river basin. The meteorological component is the first computational element by means of which rainfall input is spatially (interpolation, extrapolation) and temporally (interpolation) distributed over the basin.

Spatially and temporally distributed rainfall that falls on pervious surface is subject to losses (interception and infiltration) modelled by the rainfall loss component. In the initial and constant-rate loss method, the maximum potential rate of rainfall loss, *Lr*, is constant throughout an event. An initial loss, *Li*, represents interception and depression storage. The effective rainfall, Re_t, at time *t*, is then given by[23]:

$$Re_t = \begin{Bmatrix} 0 & \text{if } \sum R_t < Li \\ R_t - Lr & \text{if } \sum R_t > Li \text{ and } R_t > Lr \\ 0 & \text{if } \sum R_t > Li \text{ and } R_t < Lr \end{Bmatrix}, \quad (1)$$

where R_t is the rainfall depth during the time interval Δt.

The effective rainfall from the loss component contributes to direct runoff and to groundwater flow in aquifers. The Clark unit hydrograph is a frequently used technique for modelling direct runoff resulting from individual storms. In the Clark method, overland flow translation is based on a synthetic time–area histogram and the time of concentration T_c. Attenuation is modelled with a linear reservoir. The average outflow, O_t, from the reservoir during a period Δt is[23]:

$$O_t = C_A I_t + C_B O_{t-1}, \quad (2)$$

where I_t is the average inflow to basin storage, *Sb*, at time *t*, and C_A and C_B are routing coefficients given by:

$$C_A = \frac{\Delta t}{Sb + 0.5\Delta t} \quad \text{and} \quad C_B = 1 - C_A. \quad (3)$$

Both overland flow and baseflow enter river channels. The translation and attenuation of streamflow in river channels is simulated by the modified Puls method. This method can simulate backwater effects (e.g. caused by dams), can take into account floodplain storage and can be applied to a broad range of channel slopes. The modified Puls method is based on a finite difference approximation of the continuity equation, coupled with an empirical representation of the momentum equation. The continuity equation has the form[23]:

$$\left(\frac{Sc_t}{\Delta t} + \frac{O_t}{2}\right) = \left(\frac{I_{t-1} + I_t}{2}\right) + \left(\frac{Sc_{t-1}}{\Delta t} - \frac{O_{t-1}}{2}\right), \quad (4)$$

where I_t is the inflow at time *t*, O_t the outflow at time *t*, Δt the computational time step and Sc_t the channel storage at time *t*.

The movement of water in aquifers is modelled by the baseflow component. In the exponential recession model adopted in this study the baseflow at time *t*, B_t, is defined as:

$$B_t = Bi \cdot Rc^t, \quad (5)$$

where *Bi* is the initial baseflow at time t_0 and *Rc* is the exponential decay constant. A threshold flow parameter, *Td*, is added to define the point on the hydrograph where baseflow replaces overland flow as the source of flow from the sub-basin[23].

Finally, the effect of hydraulic facilities (reservoirs, detention basins) and natural depressions (lakes, ponds, wetlands) is reproduced by the reservoir component of the model. Outflow from the reservoir is computed with the level-pool routing model. The model solves recursively the following one-dimensional approximation of the continuity equation[23]:

$$I(O) = \frac{\Delta \mathrm{Sr}}{\Delta t}, \quad (6)$$

where $I(O)$ is the inflow (outflow) during the time interval Δt and ΔSr is the reservoir storage change during this interval.

A continuous version of the model is used for the analysis of periods of low flows that cause drought conditions in the basin. The continuous simulation version of the HMS model used in this study differs from the event version in the way (a) how snow accumulation and melt is accounted for and (b) how losses are calculated in the model.

The present version (v2.2.2) of HEC-HMS does not account for snow accumulation and melt processes. Since these processes are important flood-producing mechanisms in the study area, an external snow model was developed and linked with the HEC-HMS. The snow model separates spatially and temporally distributed precipitation into liquid and solid forms, and simulates solid precipitation accumulation and melt. The algorithm of the snow model is based on a degree-day method. Degree-day models are common in snowmelt modelling due to wide availability of air temperature data, good model performance and computational simplicity. In fact, most operational runoff models rely on degree-day methods for snowmelt modelling[24]. The precipitation for the time interval Δt is separated into solid (snowfall) or liquid (rainfall) form based on the average air temperature for the time interval Δt. The solid precipitation is then subject to the snow accumulation and melt algorithm. At each time interval Δt, the melted portion of snow, if any, is added to

the liquid precipitation amount. The adjusted precipitation is then used as an input into the HEC-HMS model.

Precipitation adjusted by the snow component falls on pervious and impervious surfaces of the basin. Precipitation from the pervious surface is subject to losses (interception, infiltration and evapotranspiration) modelled by the precipitation loss component. The 5-layer soil-moisture accounting (SMA) model is used to estimate and subtract the losses from precipitation. The SMA model is based on the precipitation–runoff modelling system of Leavesley *et al.*[25] and can be used for simulating long sequences of wet and dry weather periods. There are four different types of storage in the SMA model: canopy-interception storage, surface-depression storage, soil-profile storage and groundwater storage (the model can include either one or two groundwater layers). The movement of water into, out of, and between the storage layers is administered by precipitation (input into the SMA system), evapotranspiration (output), infiltration (movement of water from surface storage to soil storage), percolation (from soil storage to groundwater storage 1), deep percolation (from groundwater storage 1 to groundwater storage 2), surface runoff (output) and groundwater flow (output). For computational details of the SMA model see ref. 23. Precipitation from the impervious surface runs off with no losses, and contributes to direct runoff.

Climate modelling – weather generator

WG is recently being used as a downscaling tool in climate change studies to simulate plausible climate scenarios based on the regional observed data and GCM outputs. WGs based on the K-NN algorithm are standard, explicit and simple procedures. The K-NN algorithm typically starts with randomly selecting the current day from observed data set and a specified number of days similar in characteristics to the current day. Using resampling procedure, one of the days from the data set with similar statistical characteristics as current day is selected to represent the weather for the next day. The nearest neighbour algorithm (a) uses a simple procedure, (b) does not require major concern with the units of variables and (c) preserves well both, temporal and spatial correlation in multi-region data. Yates *et al.*[26] applied K-NN algorithm successfully with three variables (precipitation, maximum temperature and minimum temperature) to diverse areas of United States. However, the main limitation of their work is that the newly generated data stay within the range of observed minimum and maximum value.

Sharif and Burn[27] modified the K-NN WG algorithm of Yates *et al.*[26] by incorporating the perturbation process for weather variables that generates extremes outside the range of historically observed data. The modified K-NN algorithm with p variables and q stations proposed by Sharif and Burn[27] has the following steps.

(1) Calculation of regional means of p variables (x) across all q stations for each day in the historic record:

$$\bar{X}_t = [\bar{x}_{1,t}, \bar{x}_{2,t}, ..., \bar{x}_{p,t}] \quad \forall t = \{1, 2, ..., T\}, \tag{7}$$

where

$$\bar{x}_{i,t} = \frac{1}{q}\sum_{j=1}^{q} x_{i,t}^{j} \quad \forall i = \{1, 2, ..., p\}. \tag{8}$$

(2) Compute the potential neighbours of size $L = (w + 1) \times N - 1$ days long for each variable p with N years of historical record and selected temporal window of size w. All days within that window are selected as potential neighbours to the current feature vector. Among the potential neighbours, N data corresponding to the current day are eliminated in the process to prevent the possibility of generating the same value as that of the current day.

(3) Compute the regional means for all potential neighbours selected in step (2) across all q stations for each day.

(4) Compute the covariance matrix, C_t, for day t using the data block of size $L \times p$.

(5) Select randomly a value of the first time step for each variable p from all current day values in the record of N years.

(6) Compute the Mahalanobis distance expressed by eq. (9) between the mean vector of the current days ($\bar{X}_t$) and the mean vector of all nearest neighbour values ($\bar{X}_k$), where $k = 1, 2, \ldots, L$.

$$d_k = \sqrt{(\bar{X}_t - \bar{X}_k) C_t^{-1} (\bar{X}_t - \bar{X}_k)^T}, \tag{9}$$

where T represents the transpose matrix operation and C^{-1} represents inverse of covariance matrix.

(7) Select the number of $K = \sqrt{L}$ nearest neighbours out of L potential values.

(8) Sort the Mahalanobis distance d_k from smallest to largest, and retain the first K neighbours in the sorted list (they are referred to as the K nearest neighbours). Then, use a discrete probability distribution giving higher weights to closest neighbours for resampling out the set of K neighbours. The weights are calculated for each k neighbour using the following eqs (10) and (11):

$$w_k = \frac{1/k}{\sum_{i=1}^{K} 1/i}, \tag{10}$$

where $k = 1, 2, \ldots, K$. Cumulative probabilities, p_j, are given by:

$$p_j = \sum_{i=1}^{j} w_i. \tag{11}$$

Note that Sharif and Burn[27] used cumulative probability of K neighbours with eq. (11) while Yates *et al.*[26] used just a probability for each K neighbour using eq. (10).

(9) Generate random number $u(0, 1)$ and compare it to the cumulative probability p_j to determine the nearest neighbour of current day. If $p_1 < u < p_K$, then day j for which u is closest to p_j is selected. On the other hand, if $u < p_1$, then the day corresponding to d_1 is selected and if $u = p_K$, then the day corresponding to d_K is selected. Once the nearest neighbour is selected, the weather of selected day is used for all stations in the region. By this characteristic of K-NN algorithm, therefore, cross-correlation among variables in the region is preserved. In this step, improved K-NN algorithm provides the reasonable method that can randomly select one among K neighbours because it uses the cumulative probability. However in the algorithm by Yates *et al.*[26] the first nearest neighbour may be selected in most cases because it selects one of K nearest neighbours for which u is closest to a probability of each neighbour.

(10) This step is added newly by Sharif and Burn[27] to generate variables outside the range of historical data by perturbation. They suggested the optimal bandwidth (λ) that minimizes asymptotic mean integrated square error (AMISE) for a Gaussian distribution. In the univariate case, the optimal bandwidth becomes eq. (12):

$$\lambda = 1.06\sigma K^{-1/5}, \tag{12}$$

where σ represents a conditoinal standard deviation for K nearest neighbours. In addition, they suggested that a new value can be achieved from a value with mean $x_{i,t}^j$ and variance $(\lambda\sigma_i^j)^2$, i.e. the perturbation process is conducted by eq. (13):

$$y_{i,t}^j = x_{i,t}^j + \lambda\sigma_i^j z_t, \tag{13}$$

where $x_{i,t}^j$ is the value of the weather variable obtained from the original K-NN algorithm; $y_{i,t}^j$ the weather variable value from the perturbed set; z_t is normally distributed random variable with zero mean and unit variance, for day t. To prevent the negative values for bounded variables (i.e. precipitation), the largest acceptable value of $\lambda_a = x_{*,t}^j / 1.55\sigma_*^j$ is employed, where $*$ refers to a bounded weather variable[27]. If the value of the bounded weather variable computed previously is still negative, then a new value of z_t is generated.

Sharif and Burn[27] have developed the WG coded in C^{++} language employing the improved K-NN algorithm to generate three variables ($p = 3$: precipitation, maximum temperature and minimum temperature). If there are more meteorological variables available in the basin for use with the WG model, the calculation of Mahalanobis distance expressed by eq. (9) becomes quite demanding. Therefore, a modified WG model is developed that combines the modified K-NN described in the previous section with the principal component analysis (PCA), named WG-PCA. It decreases the dimension of the mean vector of the current days ($\bar{X}_t$) and the mean vector of all nearest neighbour values ($\bar{X}_k$) in step (6) by employing only the first principal component. Due to retaining of only the first principal component, multiple mechanisms may not be captured appropriately. However, this modification demonstrated a proper level of the model performance improvement. The new approach requires only the variance of the first principal component to calculate the Mahalanobis distance. The WG-PCA modifies step (6) of the algorithm presented in the previous section as follows:

(a) Calculate eigenvector and eigenvalue for the covariance matrix (C_t).
(b) Find the eigenvector related to the largest eigenvalue that explains the largest fraction of the variance described by the p variables.
(c) Calculate the first principal component with the eigenvector found in step (b) using eqs (14) and (15):

$$PC_t = \bar{\mathbf{X}}_t \mathbf{E} \tag{14}$$

$$PC_k = \bar{\mathbf{X}}_k \mathbf{E}, \tag{15}$$

where PC_t and PC_k are the values of current day and the nearest neighbour transferred by the eigenvector found in step (b) respectively and $\mathbf{E}$ the eigenvector related to the largest eigenvalue.

After calculating the PC_t and PC_k with one-dimensional matrix obtained by eqs (14) and (15), the Mahalanobis distance is computed using eq. (16):

$$d_k = \sqrt{(PC_t - PC_k)^2 / \mathrm{Var}(\mathbf{PC})} \quad \forall k = \{1, 2, ..., K\}, \tag{16}$$

where Var($\mathbf{PC}$) represents the variance of the first principal component for the K nearest neighbours.

Analysis of climate change impacts

Practical implementation of the inverse approach to the problem of high flows includes the use of a WG and an event-based hydrologic model. For a flood frequency analysis, a large number of rainfall events need to be simulated by the WG. These events are used as inputs into the hydrologic model. The outputs of the hydrologic model (peak flows) are used in frequency analysis. The application of the inverse approach to climate change impact assessment of low flows and droughts requires use of a WG model with a continuous hydrologic model. The hydrologic model adopted in this study is seasonal in nature, with a different parameter set describing summer and winter seasons.

One of the main contributions of the work presented here is the assessment of climate change impacts for a range of climate scenarios. General suggestion is to consider the assessment of impacts for three different climate scenarios. The first scenario should include the historic climate, obtained by perturbing and shuffling locally observed data for the watershed under consideration. The WG proposed in this study supports the generation of the historic climate scenario. Through the perturbation process, it allows the extreme (minimum and maximum values) generated values to be outside of the historic range. In this way, the character of the historic climate scenario reflects the existing conditions and their potential impact on the development of future climate. Two other climate scenarios named dry and wet should be derived by perturbing and shuffling historical data using inputs from GCMs. The choice of the GCMs should be made on the basis that the dry climate scenario should represent the lower boundary of potential climate change and the wet climate scenario should represent the upper boundary of potential climate change. Obviously, at different locations the names of these two scenarios may not be appropriate for describing the lower and upper boundary of climate change impacts and they should be modified accordingly. The selection of two GCMs should be made from a wide range of available models and their runs. Careful analyses of the GCM outputs should lead to the selection of only two models that will capture the potential range of climate change impacts on the watershed. Selection of the range of potential climate change through the use of two scenarios compensates for the existing level of uncertainty present in global modelling of climate change for the watershed. It is noted in the literature that the global models offer various predictions of future climate as a consequence of (i) the selected global model, (ii) the selected global model simulation scenario and (iii) the spatial and temporal resolution of the selected global model.

Dry and wet climate scenarios produced by a WG use the information provided by the outputs of two global models, as well as the locally observed data. The generated climate scenarios therefore use all available climatic data (local and global) to provide a range of future climatic conditions. It is important to point out that both wet and dry climate scenarios are equally likely as well as the range of climatic conditions between the two. Integration of the local and global data is achieved by the modification of observed data using the output of a selected GCM and then processing the modified data by the proposed WG.

Illustrative application

Detailed presentation of the application of the presented approach to the UTRB, located in southwestern Ontario, Canada is available in Prodanovic and Simonovic[22]. A brief presentation of the results is provided here. The UTRB has a drainage area of 3450 km^2 and outlets to the Lower Thames River, which is a tributary to Lake St. Clair (Figure 1). The population of the UTRB is 460,000. The main urban centre in the UTRB is the city of London, which is designated as a growth centre in the province of Ontario. Urban growth is contrasted by intensive farming in the basin. The Thames River corridors, located in a highly developed part of southwestern Ontario are vulnerable to both urban and rural land-use pressures. Despite these pressures, the Thames remains one of the most biologically diverse rivers in Canada.

Floods and droughts represent the main hydrological hazards in the UTRB. Snowmelt is a major flood-producing factor in the basin, generating flood events most frequently in March. Intensive flood-producing storms are most frequent in August. Periods of low flows usually occur during summer, and the risk of droughts is highest in July and August. Three main reservoirs in the UTRB: Fanshawe, Wildwood and Pittock, assist in flood management efforts and river flow augmentation during the drier summer months.

The area of UTRB is divided into 32 smaller sub-basins representing fine spatial resolution for semi-distributed hydrological modelling by means of the USACEs HEC-GeoHMS software (Figure 2). The meteorological component interpolates climatic input data into 32 different UTRB locations, one for each sub-basin defined as the

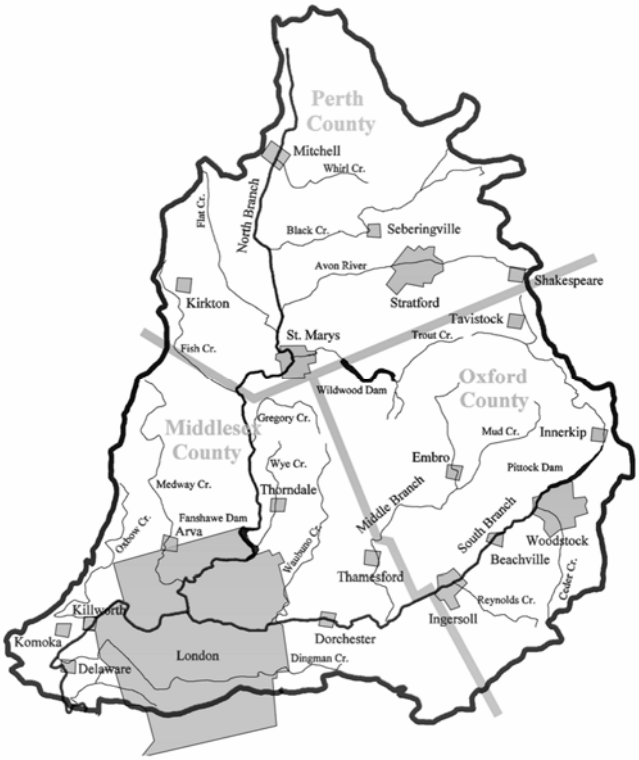

Figure 1. Map of the Upper Thames River basin (after Prodanovic and Simonovic)[22].

Table 1. Weather generator climate scenarios (after Prodanovic and Simonovic[22])

Historic	Wet (CCSRNIES B2)	Dry (CSIROM2kb B1)
Based on regional hydro-climatic data for the period 1964–2001; historic (or base case) climate.	A climate that is wetter and warmer than normal, with increased precipitation magnitude leading to higher incidents of flooding.	A climate that is drier and cooler than normal, leading to prolonged dry spells and droughts.

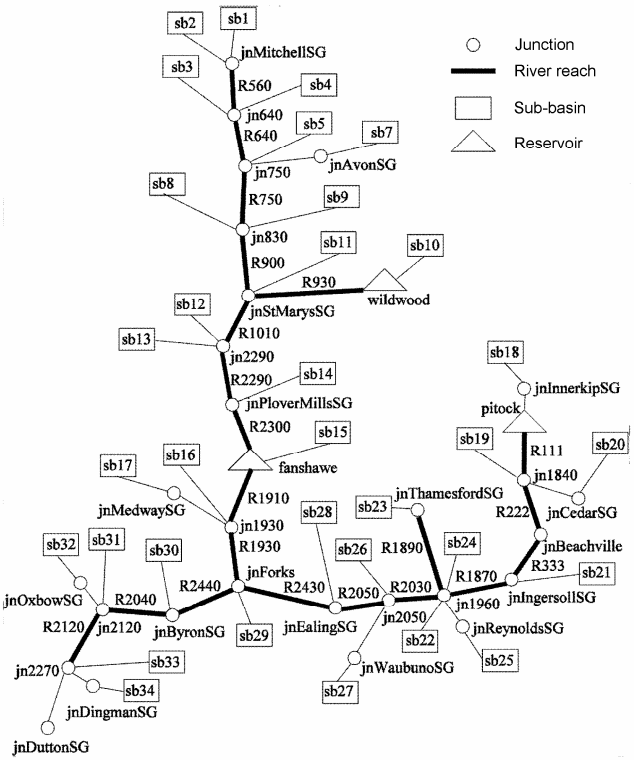

Figure 2. Schematic presentation of the Upper Thames River basin hydrologic model (after Cunderlik and Simonovic)[21].

sub-basin's centroid. The HMS model parameters are assumed to be uniform within each sub-basin.

Three different climate scenarios (Table 1) are developed for use in the UTRB. They include the historic climate, obtained by perturbing and shuffling locally observed data for the period 1964–2001. Other climate scenarios, dry and wet, are derived by perturbing and shuffling historical data using the information provided by outputs of CSIROM2kb and CCSRNIES GCMs for the grid cell containing the UTRB. The generated climate scenarios therefore use all available climatic data (local and global) to provide a range of future climatic conditions in the basin. The wet climate scenario provides conditions where emphasis is placed on increased temperature and rainfall magnitude over the next century, while the dry climate scenario emphasizes cooler and drier periods, thus providing information about future drought and drought-like conditions. The wet climate scenario is used specifically to analyse the basin's response to flooding, while the dry climate scenario (examining cooler and drier conditions) is used to assess future low flows.

The WG simulations are performed for a period of 100 years (with a daily time step) for each climate scenario and for each weather station in the area. Fifteen stations are used in the study. As there are 100 years of generated data, 100 critical events are therefore selected and used as inputs into the event hydrologic model for each climate scenario. For the analyses of low flows, the precipitation and temperature data of daily duration are produced by the WG (for historic, wet and dry climate scenarios) and used first as input into the snow accumulation and melt to provide 'adjusted' precipitation. This precipitation is then processed by the continuous hydrologic model.

Results of WG simulations are processed by the hydrologic model for historic, wet and dry climate scenarios. Annual maximum peak flows are selected from the output hydrographs and used in flood flow frequency analysis. Figure 3 shows the results of the frequency analysis for a number of gauging stations in the City of London for three simulated climate scenarios. The use of final results can be illustrated in the following way. Let us consider the results for Byron gauging station (bottom right graph in Figure 3). For one hydrologic exposure – the event that causes the dykes in the City of London to over-top (corresponding flow of 990 m^3/s). After the implementation of the inverse approach with three climate change scenarios (historic, wet and dry) we can observe that the recurrence intervals for this critical hydrologic exposure is 33 years under the historic climate, 17 years under conditions of wet climate and 65 years under the dry climate.

Figure 4 presents the results of low flow analyses in the UTRB. Again, the use of analysis results can be illustrated by focusing on the right hand graph. For one critical drought exposure – frequency of occurrence of level II drought in the vicinity of the Greenway Pollution Control Plant in Byron, we found the lowest average summer month flow to be 9.5 m^3/s. In order for level II drought to occur, the lowest average summer flow must drop to 50% of its average, to approximately 5 m^3/s. After the implementation of the inverse approach, we can observe that the recurrence intervals for this critical hydrologic exposure is 6.3 years under historic climate, 10 years under conditions of wet climate and 6.3 years under dry climate.

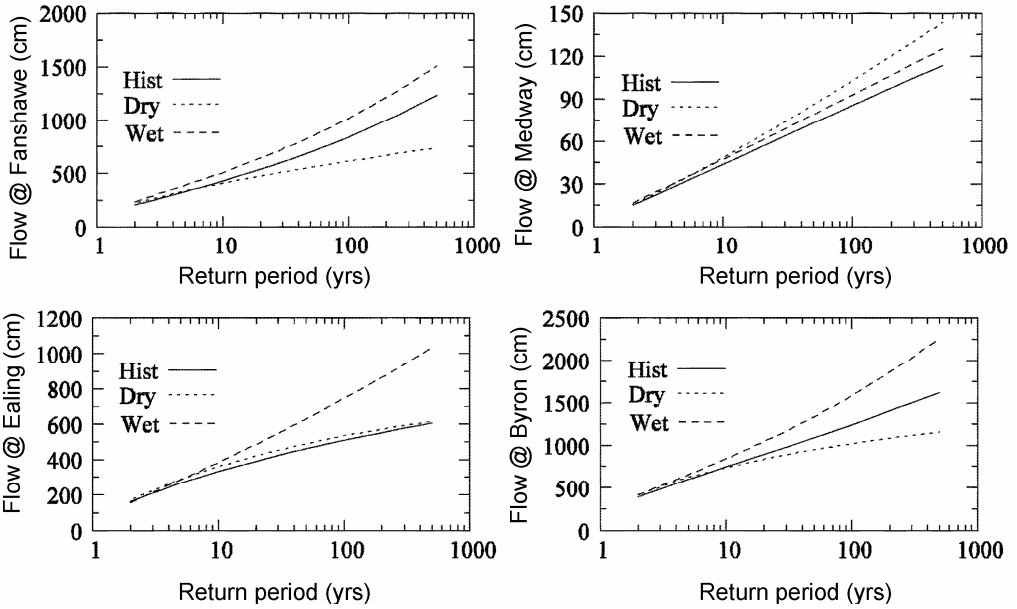

Figure 3. Flood flow analyses under climate change – the Upper Thames River basin (after Prodanovic and Simonovic)[22].

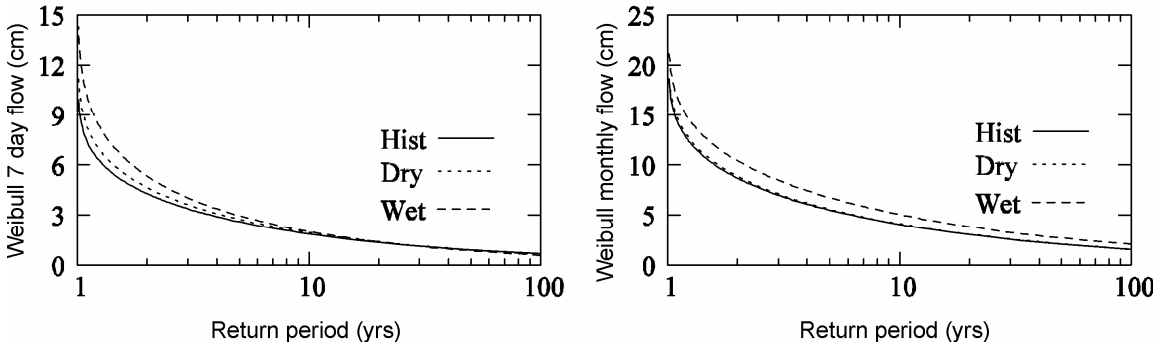

Figure 4. Low flow analyses under climate change – the Byron gauging station on the Thames River (after Prodanovic and Simonovic)[22].

Conclusions

This article presents an original approach for the assessment of climate change impacts on a local, watershed scale. The presented inverse approach starts with the analysis of existing guidelines and management practices in a watershed with respect to critical hydrological exposures that may lead to critical conditions. In the next step, the critical hydrologic exposures (flood levels for example) are transformed into corresponding critical meteorological conditions (extreme precipitation events for example). These local weather scenarios are then statistically linked to possible large-scale climate conditions that are available from the GCMs.

Two main contributions of the paper are (a) the detailed presentation of the improved WG tool by the addition of PCA; and (b) the guideline for the implementation of the inverse approach in climate change impact assessment based on the range of future climate scenarios.

The main findings obtained by the implementation of the inverse approach to the assessment of climatic change impacts in the UTRB are: (i) that flooding will occur more frequently in the future, regardless of the magnitude of floods (Figure 3) and (ii) that low flow conditions in the UTRB will remain the same as currently observed (Figure 4). Therefore, the changing climatic conditions are expected to increase flood damage in the future.

1. Prudhomme, C., Jakob, D. and Svensson, C., Uncertainty and climate change impact on the flood regime of small UK catchments. *J. Hydrol.*, 2003, **277**, 1–23.
2. Meehl, G. A. and Tebaldi, C., More intense, more frequent, and longer lasting heat waves in the 21st century. *Science*, 2004, **305**, 994–997.
3. Intergovernmental Panel on Climate Change (IPCC), *Climate Change and Water*. Bates, Bryson, Kundzewicz, Zbigniew, W., Wu, Shaohong and Palutikof, Jean. Technical Paper VI of the Intergovernmental Panel on Climate Change, 200, Geneva, Switzerland, IPCC Secretariat, 2008.

4. Hansen, J. *et al*., Target atmospheric CO_2: where should humanity aim? *Open Atmos. Sci. J*., 2008, **2**, 217–231.
5. Rahmstorf, S. *et al.*, Recent climate observations compared to projections. *Science*, 2007, **316**, 709.
6. Li, L. and Simonovic, S. P., System dynamic model for predicting floods from snowmelt in North American Prairie watersheds. *Hydrol. Proc*., 2002, **16**, 2645–2666.
7. Eckhardt, K. and Ulbrich, U., Potential impacts of climate change on groundwater recharge and streamflow in a central European low mountain range. *J. Hydrol.*, 2003, **284**, 244–252.
8. Lemmen, D. S. and Warren, F. J. (eds), *Climate Change Impacts and Adaptation: A Canadian Perspective*, Natural Resources Canada, 2004, p. 201.
9. Koshida, G. and Avis, W., *Canada Country Study: Climate Impacts and Adaptation*, Vol. VII, National Sectoral Volume. Environment Canada, Ottawa, 1998.
10. Gan, T. Y., Finding trends in air temperature and precipitation for Canada and North-Eastern United States. In *Using Hydrometric Data to Detect and Monitor Climatic Change* (eds Kite, G. W. and Harvey, H. D.), Proceedings of NHRI Workshop No. 8, National Hydrology Research Institute, Saskatoon, SK, 1992, pp. 57–78.
11. Whitfield, P. H. and Cannon, A. J., Recent variations in climate and hydrology in Canada. *Can. Water Resour. J.*, 2000, **25**, 19–65.
12. Zhang, X., Vincent, L. A., Hogg, W. D. and Niitsoo, A., Temperature and precipitation trends in Canada during the 20th century. *Atmos. Ocean*, 2000, **38**, 395–429.
13. Zwiers, F. W. and Kharin, V. V., Changes in the extremes of the climate simulated by CCC GCM2 under CO_2 doubling. *J. Climate*, 1998, **11**, 2200–2222.
14. Zhang, X., Harvey, K. D., Hogg, W. D. and Yuzyk, T. R., Trends in Canadian streamflow. *Water Resour. Res*., 2001, **37**, 987–998.
15. Mote, P. W., Twentieth-century fluctuations and trends in temperature, precipitation, and mountain snowpack in the Georgia Basin – Puget Sound Region. *Can. Water Resour. J*., 2003, **28**, 567–585.
16. Roy, L., Leconte, R., Brissette, F. P. and Marche, C., The impact of climate change on seasonal floods of a southern Quebec River Basin. *Hydrol. Proc*., 2001, **15**, 3167–3179.
17. Hengeveld, H., *Projections for Canada's Climate Future*, Climate Change Digest 00-01, Environment Canada, Ottawa, ON, 2000.
18. Mitchell, J. G., Down the drain? The incredible shrinking Great Lakes. *Nat. Geogr*., 2002, pp. 37–51.
19. Environment Canada, Threats to water availability in Canada. National Water Research Institute, Burlington, Ontario. NWRI Scientific Assessment Report Series No. 3 and ASCD Science Assessment Series No. 1, 2004, p. 128.
20. Cunderlik, J. and Simonovic, S. P., Hydrologic extremes in southwestern Ontario under future climate projections. *J. Hydrol. Sci.*, 2005, **50**, 631–654.
21. Cunderlik, J. and Simonovic, S. P., Inverse flood risk modeling under changing climatic conditions. *Hydrol. Proc. J*., 2007, **21**, 563–577.
22. Prodanovic, P. and Simonovic, S. P., Impacts of changing climatic conditions in the Upper Thames River basin. *Can. Water Resour. J*., 2007, **32**, 265–284.
23. USACE, Hydrologic Modeling System HEC-HMS. *Technical Reference Manual*, US Army Corps of Engineers, Hydrologic Engineering Centre, 2000.
24. Hock, R., Temperature index melt modeling in mountain areas. *J. Hydrol*., 2003, **282**, 104–115.
25. Leavesley, G. H., Lichty, R. W., Troutman, B. M. and Saindon, L. G., *Precipitation–runoff Modeling System User's Manual*, Water-Resources Investigations, 83-4238, US Dept of the Interior, Geological Survey, Denver, CO, 1983.
26. Yates, D., Gangopadhyay, S., Rajagopalan, B. and Strzepek, K., A technique for generating regional climate scenarios using a nearest-neighbor algorithm. *Water Resour. Res*., 2003, **39**, 7–14.
27. Sharif, M. and Burn, D. H., Simulating climate change scenarios using an improved K-nearest neighbor model. *J. Hydrol.*, 2006, **325**, 179–196.

ACKNOWLEDGEMENTS. Work presented in this paper is the product of a team collaboration. I thank Juraj Cunderlík, Predrag Prodanovic, Shawn Gettler, Mark Helsten, Matt Wood, Linda Mortsch, Andrea Hebb, Donald Burn, Mohammed Sharif, Karen Wey and Hyung-Ill Eum for their assistance.